Activated carbon embedded alginate beads for removing nonsteroidal anti-inflammatory drug naproxen from wastewater: equilibrium, kinetics, thermodynamics, desorption, and reusability

Nazli Ozcan and Didem Saloglu

ABSTRACT

In the present study, activated carbon/alginate (AC/ALG) beads were successfully synthesized with different AC:ALG ratios of 1.0–3.0 (w/v) and used for the adsorption of the nonsteroidal anti-inflammatory drug naproxen from wastewater. The beads were characterized by Fourier transform infrared spectroscopy (FT-IR), scanning electron microscopy (SEM), and Brunauer–Emmett–Teller (BET) analysis, and adsorbent dosage, initial pH, initial naproxen concentration, and contact time in removal efficiency were investigated. Maximum naproxen removal percentage was achieved using 350 mg of AC/ALG beads with a ratio of 3.0% (w/v) within six hours and naproxen removal performance was determined to be 98.0%. Freundlich, Temkin, and Dubinin–Radushkevich (D-R) isotherm models were fitted to the equilibrium data better than the Langmuir model. According to kinetics results, the equilibrium time for the AC/ALG beads was reached in four hours and the kinetic model was determined by the pseudo-second-order equation. The thermodynamic parameters were calculated and enthalpy of naproxen adsorption was found to be positive for all AC/ALG beads. After the adsorption process the beads can easily be regenerated by ethanol and reused within seven cycles.

Key words | alginate, isotherm, kinetics, naproxen, reusability, thermodynamics

Nazli Ozcan
Yesilyurt Demir Celik Vocational School,
Department of Chemical Technologies,
Ondokuz Mayis University,
Samsun,
Turkey
and
Institute of Science, Department of Chemical Engineering,
Yalova University,
Yalova,
Turkey

Didem Saloglu (corresponding author)
Faculty of Engineering, Department of Chemical Engineering,
Yalova University,
Yalova,
Turkey
E-mail: *didemsalogludertli@gmail.com*

HIGHLIGHTS

- Adsorption of nonsteroidal anti-inflammatory drug naproxen by activated carbon embedded alginate beads was investigated.
- Activated carbon embedded alginate beads effectively eliminated 98.0% of the naproxen.
- Equilibrium adsorption data of naproxen onto the beads were well represented by the Freundlich, Temkin, and D-R models.
- The adsorption kinetic data were well described by the pseudo-second-order model.
- Thermodynamic study showed that the naproxen adsorption process was spontaneous and endothermic under study conditions.

doi: 10.2166/wst.2020.196

GRAPHICAL ABSTRACT

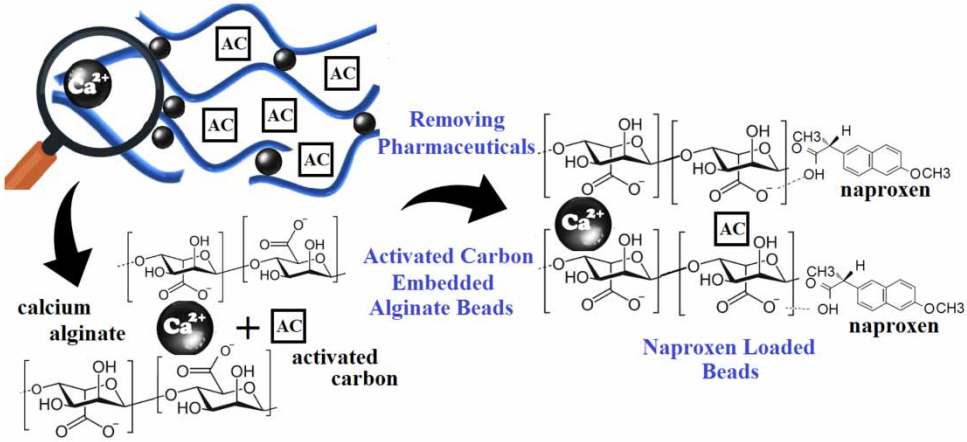

INTRODUCTION

Pharmaceutical compounds belong to the most important groups of emerging pollutants noticed in water sources. Non-steroidal anti-inflammatory drugs illustrate one of the most commonly used pharmaceuticals available without a prescription and usage of these drugs has increased in recent years. These compounds are frequently detected in surface water, wastewater, groundwater, and domestic water. Furthermore, pharmaceutical pollution has been an increasingly important subject for researchers over the past decade (Khazri *et al.* 2017; Simsek *et al.* 2017; Ahmed & Hameed 2018).

The most-often detected drugs in various water sources, naproxen, ciproflaxin, diclofenac, ibuprofen, and carbamazepine, are widely used in medicine as analgesic, anti-inflammatory and antipyretic agents. These pharmaceuticals are considered a high environmental risk, even if they appear in water in the range of mgL^{-1} and μgL^{-1}, and are removed in conventional wastewater treatment plants with low efficiency (Larous & Meniai 2016; Kooijman *et al.* 2020).

Naproxen is commonly used for human health as a non-steroidal anti-inflammatory drug for the relief of symptoms of rheumatoid arthritis and osteoarthritis. Despite the lack of determining naproxen, its presence is monitored in surface water, groundwater, wastewater, and domestic water. Naproxen at mgL^{-1} levels in wastewater and domestic water has the potential to cause negative health effects, and removal of the drug from these waters is an important subject for researchers (Reynel-Avila *et al.* 2015).

Although various conventional methods, such as coagulation, flocculation, biodegradation, and photodegradation, have been adopted in separation techniques, these methods have not been effectively used for pharmaceutical compounds (Kooijman *et al.* 2020). Analysis of the various methods of removing pharmaceuticals shows there is high efficiency in using adsorption processes (Ahmed & Hameed 2018). Adsorption of pharmaceuticals has been studied mainly in batch/continuous conditions using carbon-based adsorbents such as activated carbon, carbon fibre, carbon nanotubes, etc. due to their high surface areas and pore size distributions. Among carbon-based materials, activated carbon has attracted increased attention with its high adsorption capacity, chemical stability, and feasibility of production. Considering environmental concerns, biopolymers have also attracted great interest for use as adsorbents in wastewater treatment. One biopolymer – alginate – is a natural, linear polysaccharide that has been applied in a variety of micropollutants such as pharmaceuticals and food and textile dyes, and is frequently used as an adsorbent for heavy metal removal (Larosa *et al.* 2018). Carbon-containing polymeric biocomposites with high adsorption capacity have been precursors in the search for new adsorbents in recent decades (İlbay *et al.* 2015). Therefore, embedding activated carbon into the alginate's molecular structure can significantly increase the surface area and pore size of the polymer and improve the adsorption capacity of the alginate; meanwhile, a new adsorbent can be designed for the removal of pharmaceuticals from wastewater.

The aim of this work is to synthesize and characterize activated carbon embedded alginate (AC/ALG) beads as a novel adsorbent for removing pharmaceuticals from wastewater. The effects of various parameters, such as pH, amount of adsorbent, time, and temperature, were analysed for adsorption of the non-steroidal anti-inflammatory drug naproxen. Langmuir, Freundlich, Temkin, and Dubinin–Radushkevich (D-R) adsorption isotherm models, pseudo-first-order, pseudo-second-order, Elovich, Weber–Morris, and Bangham kinetic models, adsorption thermodynamic, mechanism, desorption, and reusability studies were also carried out. It can be safely stated that this work represents the first in the literature to follow the adsorption behaviour of AC/ALG beads for naproxen. AC/ALG beads have considerable potential in the adsorption of pharmaceutical compounds from wastewater.

MATERIALS AND METHODS

Materials

Sodium alginate was purchased from Acros Organics; naproxen, NaCl, and $CaCl_2$ were produced by Sigma Aldrich; ethanol, methanol, HCl, and NaOH were supplied by Merck; and activated carbon with 850 $m^2 g^{-1}$ surface area was obtained from Zag Industrial Chemicals. All reagents were of analytical grade chemicals and used as received.

Preparation of alginate and activated carbon embedded alginate beads

A solution of 2% (w/v) sodium alginate was prepared by mixing 2.0 g of sodium alginate powder with 100 mL of 0.1 M NaCl solution to obtain raw ALG solution. AC was added to the ALG solution with different AC:ALG ratios of 1.0–3.0% (w/v) to synthesize AC/ALG:(1.0–3.0) solutions (Simsek *et al.* 2017). The solutions were stirred with a magnetic stirrer until homogeneous mixtures were obtained. After homogenization, the mixtures were added dropwise to 0.1 M $CaCl_2$ solution using a 1 mL plastic syringe and left with a magnetic stirrer for 24 h (Hu *et al.* 2018). The formed raw ALG and AC/ALG beads were gently separated from the gelling medium and washed with distilled water. Finally, the beads were dried in an oven at 60 °C for 24 h.

Characterization of beads

The molecular structures of raw AC, raw ALG, and AC/ALG beads were determined by a Perkin Elmer spectrometer (Simsek *et al.* 2017). N_2 adsorption measurements were performed using a Micromeritics ASAP 2020 surface analyser. The specific surface area and pore volumes were specified by the Brunauer–Emmett–Teller (BET) method. The morphology of the beads was determined by scanning electron microscopy (ESEM-FEG/EDAX Philips XL-30) (Li *et al.* 2017). The points of zero charges (PZC) of raw ALG, raw AC, and AC/ALG beads were established using the salt addition method (Saloglu & Ozcan 2018).

Preparation and determination of naproxen solution

Naproxen stock solution was prepared using distilled water and naproxen concentration was detected using a UV-vis spectrophotometer (Shimadzu UV1800) at 230 nm wavelength (Saloglu & Ozcan 2018). The UV absorption spectra of naproxen solution prepared at 2–100 mgL^{-1} were recorded against distilled water and the calibration curve was obtained as $R^2 = 0.99$.

Preliminary adsorption experiments

An amount of 25 mL of 50 mgL^{-1} naproxen solution in distilled water with pH from 3.0 to 11.0 was added to 100–500 mg of AC/ALG:(1.0–3.0) beads in a 100 mL Erlenmeyer at 25, 45, and 60 ± 0.5 °C and batch adsorption experiments were done on a mechanical shaker at 140 rpm for six hours. The beads were separated from the naproxen solution and absorbance values of the supernatants were measured using the UV-vis spectrophotometer. Each experiment was duplicated under identical conditions and average results were reported.

The adsorption capacity of naproxen, q_e (mgg^{-1}), was calculated by Equation (1):

$$q_e = \frac{(C_i - C_e)}{m} V \quad (1)$$

where q_e is adsorption capacity (mgg^{-1}), V is solution volume (L), m is adsorbent dosage (g), and C_i and C_e are initial and equilibrium concentrations (mgL^{-1}), respectively.

Adsorption isotherms of naproxen onto raw AC, raw ALG, and AC/ALG:(1.0–3.0) beads were defined by different models, namely Langmuir, Freundlich, D-R, and Temkin. The isotherms were studied in 50 mgL^{-1} naproxen solution with 100–500 mg of AC/ALG:(1.0–3.0) beads at pH 5.0. Similarly, adsorption kinetics experiments were performed using 50 mgL^{-1} naproxen solution and 350 mg of beads for different time intervals and adsorption kinetics

were determined by pseudo-first-order, pseudo-second-order, Elovich, Weber–Morris, and Bangham models (Khazri *et al.* 2017). The batch adsorption experiments were carried out at 25, 45, and 60 ± 0.5 °C in order to examine the thermodynamic properties of adsorption.

Desorption studies were conducted by suspending naproxen-loaded AC/ALG:3.0 beads in distilled water, ethanol, and methanol (Seo *et al.* 2016). Firstly, 350 mg of beads were added to 50 mgL^{-1} naproxen solutions. Naproxen-loaded beads, distilled water, and other solutions were shaken at 25 °C for five hours at 140 rpm and the residual naproxen concentration was measured spectrophotometrically. Desorption efficiency was calculated as the ratio of desorbed amount to adsorbed amount of naproxen.

Ten cycles of consecutive adsorption–desorption studies (Ogata *et al.* 2017) in ethanol were carried out in order to check the reusability of AC/ALG:3.0 beads. The beads were added to 50 mgL^{-1} naproxen solution and the obtained suspension was shaken at 25 °C for 5 h at 140 rpm. Subsequently, the suspension was filtered and naproxen concentration was measured spectrophotometrically. After adsorption, the naproxen-loaded beads were collected, dried, and then used for the desorption experiment. The collected beads were added to 50 mL ethanol and the suspension was shaken at 25 °C for 5 h at 140 rpm. Then, the suspension was filtered and the concentration of naproxen was measured again.

RESULTS AND DISCUSSION

Characterization of beads

Fourier transform infrared spectroscopy (FT-IR) analysis was performed to determine the functional groups of raw AC, raw ALG, and AC/ALG beads in the range of 650 and 3,650 cm^{-1} (Figure 1(a)). The FT-IR spectrum showed significant peaks of raw ALG beads. The broad absorption peak near 3,300 and 2,950 cm^{-1} represented O-H groups and aliphatic C-H stretching (Simsek *et al.* 2017). The characteristic peaks at 1,610 and 1,450 cm^{-1} were attributed to asymmetric and symmetric C = O bonds (from COO^{-}),

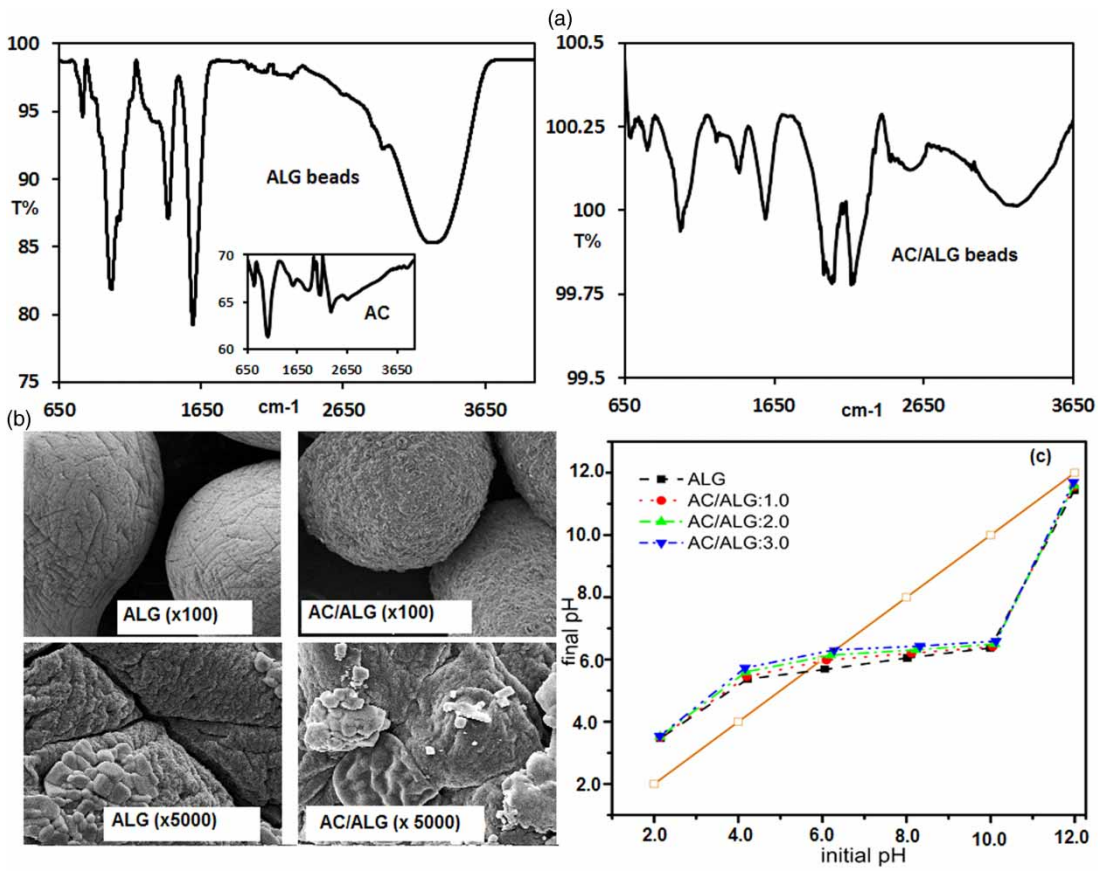

Figure 1 | (a) FT-IR, (b) SEM analysis, and (c) PZC values of AC, ALG, and AC/ALG beads.

respectively. The main bands positioned around 1,095, 1,075, and 1,035 cm^{-1} indicated the vibration of the C-O band, stretching vibration of C-C, and C-C bending of raw alginate beads (Larosa *et al.* 2018). Furthermore, the AC/ALG beads exhibited a very different spectrum in comparison with the AC and ALG beads. The absorption region of the stretching vibration of O-H bonds and asymmetric and symmetric C = O bonds in the AC/ALG beads appeared at much lower intensity than in raw ALG. The change in the bands is strong evidence of the interaction between AC and ALG and it can be safely mentioned that AC/ALG beads were successfully synthesized.

The scanning electron microscopy (SEM) images of raw ALG and AC/ALG beads are given in Figure 1(b). As is seen, the raw ALG surface was full of long microfractures; numerous microfractures (ca. 500 μm) entirely covered the ALG surface and provided a uniform area. This morphology made raw ALG very attractive for AC embedding into the microfractures. When focused on the surface of AC/ALG beads (×5000), agglomeration of AC on the ALG surface was clearly seen. This structure is evidence of the interaction of AC and ALG in molecular structure. Furthermore, the presence of AC on the ALG beads led to the formation of a large number of potential active sites and receptive regions, and, thus, increased naproxen adsorption. On the basis of comparison between SEM images of raw ALG and AC/ALG beads, a new surface morphology created by AC placed onto the ALG made its surface attractive for naproxen adsorption (Larosa *et al.* 2018).

The results obtained from SEM images were also supported by BET analysis (Li *et al.* 2017). The specific surface areas of raw ALG, raw AC, and AC/ALG:(1.0–3.0) were 138, 850, 246, 327, and 418 $m^2 g^{-1}$, respectively, and they were listed as AC > AC/ALG:3.0 > AC/ALG:2.0 > AC/ALG:1.0. In addition, total pore volumes were raised by introducing AC into raw ALG. AC represented the largest total pore volume; therefore, larger pores were formed on AC/ALG beads. The total pore volume values were found to be 0.158, 0.214, and 0.278 $cm^3 g^{-1}$ for AC/ALG:1.0, AC/ALG:2.0, and AC/ALG:3.0, respectively. The restoration of the surface properties of raw ALG was explained by the part of AC performance as a supporting material.

Preliminary adsorption experiments

The point of zero charge for raw AC, raw ALG, and AC/ALG beads is represented in Figure 1(c). The raw ALG beads had a positive surface when solution pH was lower than 5.6, owing to the presence of the -COOH groups of the beads. PZC values of raw AC and AC/ALG:(1.0–3.0) beads were also determined as 7.0, 5.8, 6.2, and 6.3, respectively. The PZC values of AC/ALG:(1.0–3.0) beads increased after embedding AC due to deprotonated carboxylic acids of the alginate. The PZC values of AC/ALG:(1.0–3.0) beads stated that when solution pH ranged from 6.0 to 14.0, the surfaces of the beads were negative, and when pH was below 6.0 the surfaces were positive (Saloglu & Ozcan 2018).

Figure 2(a) and 2(b) represent the effect of pH and the amount of beads on naproxen adsorption. The results showed that naproxen adsorption capacity (q_e) of raw AC, raw ALG, and AC/ALG:(1.0–3.0) beads decreased sharply with rising pH from 3.0 to 11.0 (Figure 2(a)). The q_e values detected were much higher (nearly 1.75-fold) at acidic and neutral solution pHs rather than basic pHs. The maximum q_e values were determined to be nearly 3.5 mgg^{-1} for raw AC and AC/ALG:(1.0–3.0) beads when solution pH was between 3.0 and 7.0. Furthermore, q_e values for raw AC and AC/ALG:3.0 beads declined from 3.7 and 3.4 mgg^{-1} to 2.5 and 2.2 mgg^{-1}, with an increasing pH from 5.0 to 11.0, respectively (Figure 2(a)). A convincing explanation of the effect of pH on naproxen adsorption could be that O-H, C-O, and C = O groups of the AC/ALG beads were responsible for the adsorption of naproxen in acidic and neutral solution pHs due to the anionic groups that influenced the interactions between the beads and naproxen. In addition, considering that the pKa value of naproxen is 4.15, naproxen molecules become negatively charged if the solution pH is above this value (Yu *et al.* 2008). Therefore, at pH 9.0 and 11.0, a repulsion of naproxen and AC/ALG beads existed, resulting in decreased interactions. When the pH was boosted to 9.0 and 11.0, a great number of

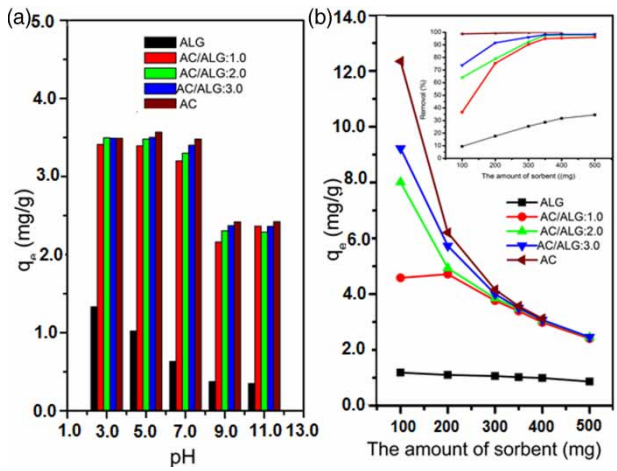

Figure 2 | Effect of (a) pH and (b) adsorbent amount on naproxen adsorption onto AC, ALG, and AC/ALG beads.

O-H groups in the solution competed with negative groups of naproxen to attain the active sites of the beads; this assertive competition could reduce the adsorption capacity. To sum up, when pH was between 3.0 and 7.0, the surfaces of all beads were positively charged, which adsorbed the O-H groups of naproxen using hydrogen bonds. The maximum adsorption capacities were determined below neutral pHs; therefore, pH 5.0 was selected as the optimum pH value for naproxen adsorption.

Figure 2(b) displays the effect of adsorbent amount on adsorption capacities and removal % of naproxen using raw AC, raw ALG, and AC/ALG:(1.0–3.0) beads. The q_e values and naproxen adsorption percentages were determined as 12.3, 9.2, and 1.2 mgg^{-1}, and 98.7%, 73.8%, and 9.5% for 100 mg raw AC, AC/ALG:3.0, and raw ALG, respectively. Moreover, removal % and q_e values were detected as 29.0%, 95.0%, 97.4%, 98.0%, and 99.6%, and 1.0, 3.4, 3.5, 3.5, and 3.56 mgg^{-1} using 350 mg of raw ALG, AC/ALG:1.0, AC/ALG:2.0, AC/ALG:3.0, and raw AC, respectively. According to Figure 2(b), as the amount of AC in the beads increased, naproxen removal percentages were effectively boosted. This is because the AC enhanced the specific surface area and active sites of the AC/ALG beads, as described in BET and SEM analysis (Li *et al.* 2017).

Adsorption isotherms

The equilibrium adsorption isotherms of naproxen using raw AC, raw ALG, and AC/ALG:(1.0–3.0) beads are presented in Figure 3. The relationship between naproxen adsorption and the equilibrium concentrations is described by Langmuir, Freundlich, Temkin, and D-R isotherm models (Önal *et al.* 2007; Zhou & Zhou 2014). The model parameters were calculated from the slope and intercept of the plots; the parameters and correlation coefficients (R^2) of naproxen adsorption onto raw ALG, raw AC, and AC/ALG beads are shown in Table 1.

The R_L values of the Langmuir model were determined as 0.03 Lmg^{-1} for raw AC, 0.50 Lmg^{-1} for raw ALG, and 0.03 Lmg^{-1} for AC/ALG:3.0 beads; these values were less than 1.0. Of note is that naproxen adsorption fits the Langmuir model. R^2 values were between 0.80 and 0.94, and the model characterized naproxen adsorption according to R^2 values. Despite the R_L and R^2 values being suitable for fitting the model, $q_{m,model}$ and $q_{m,experiment}$ values were found to be 36.7 mgg^{-1} and 3.56 mgg^{-1}; 2.70 mgg^{-1} and 1.02 mgg^{-1}; 4.82 mgg^{-1} and 3.39 mgg^{-1}; 6.27 mgg^{-1} and 3.48 mgg^{-1}; and 7.81 mgg^{-1} and 3.50 mgg^{-1} for raw AC, raw ALG, and AC/ALG:(1.0–3.0), respectively (Table 1). The Langmuir model was not suitable for naproxen adsorption due to the difference between the q_e values calculated from the model and experiments.

The Freundlich isotherm model is suitable for adsorption appearing on a heterogeneous surface. The isotherm declares surface heterogeneity as well as active site distribution of adsorbents. K_F and $1/n$ demonstrate relative adsorption capacity and the heterogeneity factor of the adsorbents, respectively. The value of $1/n$ signifies the adsorption is favourable when $1/n < 1.0$, difficult when $0.5 < 1/n < 1.0$, and unfavourable when $1/n > 1.0$ (Zhou & Zhou 2014). The values of K_F and $1/n$ were calculated as 12.57 mgg^{-1} and 0.48 for AC, and 3.34 mgg^{-1} and 0.52 for AC/ALG:3.0 beads, as shown in Table 1. For naproxen adsorption onto raw AC, raw ALG, and AC/ALG:(1.0–3.0), $1/n$ values were lower than 1.0, so the Freundlich model was favourable for naproxen adsorption. The R^2 values of the model ranged between 0.83 and 0.97, which are higher than that of the Langmuir model (Table 1). The Freundlich model can be used effectively for the adsorption.

The Temkin isotherm model considers that the heat of adsorption declines linearly while active sites of the adsorbent are enclosed by adsorbate molecules; the model accepts adsorbate–adsorbent interaction (Dada *et al.* 2012). A_T values were calculated as 8.90, 0.13, 5.80, 4.10, and 3.54 Lmg^{-1} for raw AC, raw ALG, and AC/ALG:(1.0–3.0), respectively. Furthermore, the heat of adsorption (B) was found to be 6.42–0.99 $Jmol^{-1}$ for raw AC and AC/ALG:3.0. Based on the R^2 values (between 0.81 and 0.99), this model fitted the equilibrium data well.

The D-R isotherm model assumes an adsorption mechanism with Gaussian energy distribution onto a heterogeneous surface with a multilayer physical adsorption mechanism (Inyınbor *et al.* 2016). The values of $q_{m,model}$ and β were calculated as 22.41 $molg^{-1}$ and 1×10^{-7} mol^2KJ^{-2}; 1.48 $molg^{-1}$ and 8×10^{-5} mol^2KJ^{-2}; 4.54 $molg^{-1}$ and 5×10^{-7} mol^2KJ^{-2}; 6.41 $molg^{-1}$ and 9×10^{-7} mol^2KJ^{-2}; and 7.87 $molg^{-1}$ and 6×10^{-7} mol^2KJ^{-2} for raw AC, raw ALG, and AC/ALG:(1.0–3.0) beads, respectively. The coefficient of determination calculated between 0.70 and 0.98 indicated a poor fit compared with the Freundlich model. E is the adsorption mean free energy, and adsorption is accepted as physical adsorption if $E < 8$ $kJmol^{-1}$; it is called chemisorption if 8 $kJmol^{-1} < E < 16$ $kJmol^{-1}$. The mean free energies of all beads were determined to be lower than 8 $kJmol^{-1}$, which declared that the naproxen adsorption occurred physically.

Based on the correlation coefficients (R^2) and $q_{m,model}$ values, the parameters of the Freundlich, Temkin and D-R models fitted the naproxen adsorption better than the

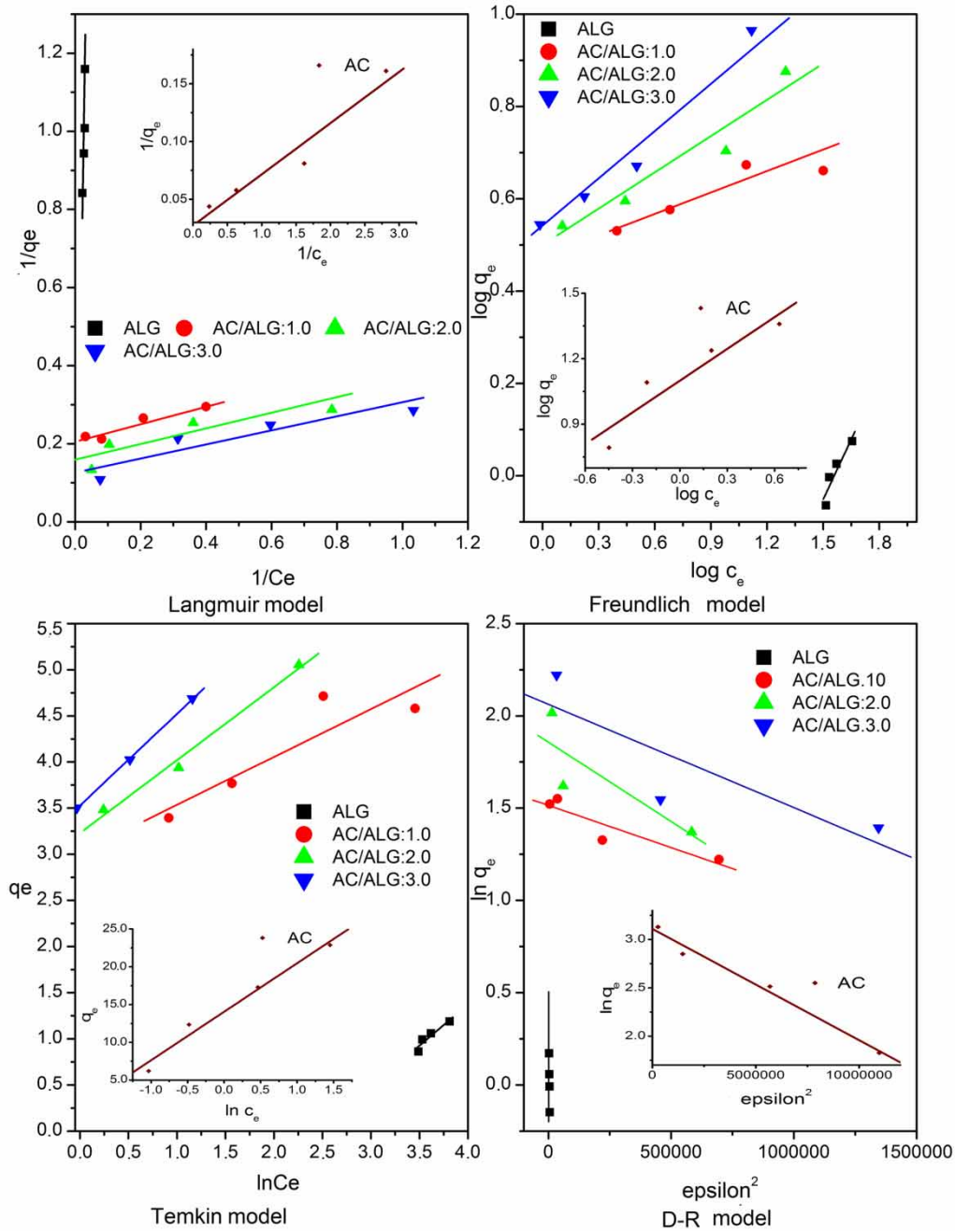

Figure 3 | Adsorption isotherm models of naproxen onto AC, ALG, and AC/ALG beads.

Langmuir model. According to the outcome of studying all these models, naproxen adsorption can be said to form on multilayer heterogeneous bead surfaces. The active sites of the beads increased logarithmically during the adsorption process because of the resulting multilayer adsorption and heterogeneous pore distribution. Moreover, adsorption heat diminished linearly while the active sites of the beads were fully covered by naproxen molecules and adsorption occurred by a uniform bonding energy.

Adsorption kinetics

The kinetic profiles containing the equilibrium adsorption capacity values versus time are shown in Figure 4. The

Table 1 | Adsorption isotherm model parameters of naproxen onto AC, ALG, and AC/ALG beads

	AC	ALG	AC/ALG:1.0	AC/ALG:2.0	AC/ALG:3.0
Langmuir isotherm model	$\frac{1}{q_e}=\frac{1}{q_m b}\frac{1}{C_e}+\frac{1}{q_m}$				
	$R_L=\frac{1}{(1+C_e b)}$				
$q_{e\text{-experimental}}$ (mgg^{-1})	*3.56*	*1.02*	*3.39*	*3.48*	*3.50*
$q_{m,model}$ (mgg^{-1})	36.7	2.70	4.82	6.27	7.81
b	0.6	0.017	0.96	0.88	0.75
R_L (Lmg^{-1})	0.03	0.50	0.02	0.02	0.03
R^2	0.94	0.93	0.90	0.80	0.84
Freundlich isotherm model	$q_e=K_F C_e^{1/n}$				
K_F (mgg^{-1})	12.57	8.24	3.10	3.10	3.34
$1/n$	0.48	0.59	0.13	0.49	0.52
R^2	0.88	0.90	0.83	0.93	0.97
Temkin isotherm model	$q_e=\frac{RT\ln(K_t C_e)}{b_T}$				
	$B=\frac{RT}{b_T}$				
A_T (Lmg^{-1})	8.90	0.13	5.80	4.10	3.54
B ($Jmol^{-1}$)	6.42	0.66	0.52	0.79	0.99
R^2	0.97	0.97	0.81	0.98	0.99
D-R isotherm model	$\ln q_e=\ln q_m-\beta(\varepsilon)^2$				
	$(\varepsilon)=RT\ln\left(1+\frac{1}{C_e}\right)$				
	$E=\frac{1}{\sqrt{2\beta}}$				
$q_{e\text{-experimental}}$ (mgg^{-1})	3.56	1.02	3.39	3.48	3.50
q_{model} ($molg^{-1}$)	22.41	1.48	4.54	6.41	7.87
β (mol^2KJ^{-2})	1E-07	8E-05	5E-07	9E-07	6E-07
E ($kJmol^{-1}$)	3.31	0.07	0.83	1.43	1.76
R^2	0.98	0.96	0.84	0.70	0.72

adsorption kinetic curve of naproxen on all adsorbents showed that adsorption reached equilibrium after four hours and remained constant until the end of the experiment. Naproxen adsorption onto raw AC, raw ALG, and AC/ALG:(1.0–3.0) beads was quite fast during the first 100 minutes, then continued at a slower adsorption rate, and then reached equilibrium at the end of the four hours; C_e and q_e values were found to be 39.8 mgL^{-1} and 0.72 mgg^{-1}; 0.50 mgL^{-1} and 3.53 mgg^{-1}; 5.65 mgL^{-1} and 3.16 mgg^{-1}; 5.05 mgL^{-1} and 3.25 mgg^{-1}; and 4.96 mgL^{-1} and 3.35 mgg^{-1} for raw ALG, raw AC, and AC/ALG:(1.0–3.0) beads in this period, respectively (Figure 4). In addition, q_e and removal % values were measured as 3.56 mgg^{-1} and 99.6%; 0.79 mgg^{-1} and 29.0%; 3.34 mgg^{-1} and 94.0%; 3.36 mgg^{-1} and 94.0%; and 3.49 mgg^{-1} and 98.0% for raw ALG, raw AC, and AC/ALG:(1.0–3.0) beads, respectively, in six hours.

The adsorption kinetics were described using pseudo-first-order, pseudo-second-order, Weber–Morris, Elovich, and Bangham models. The pseudo-first-order model can be applied to solid–liquid adsorption, the pseudo-second-order model accepts chemisorption, the Weber–Morris intraparticle diffusion model explains mass transfer phenomena during the adsorption process, the Elovich

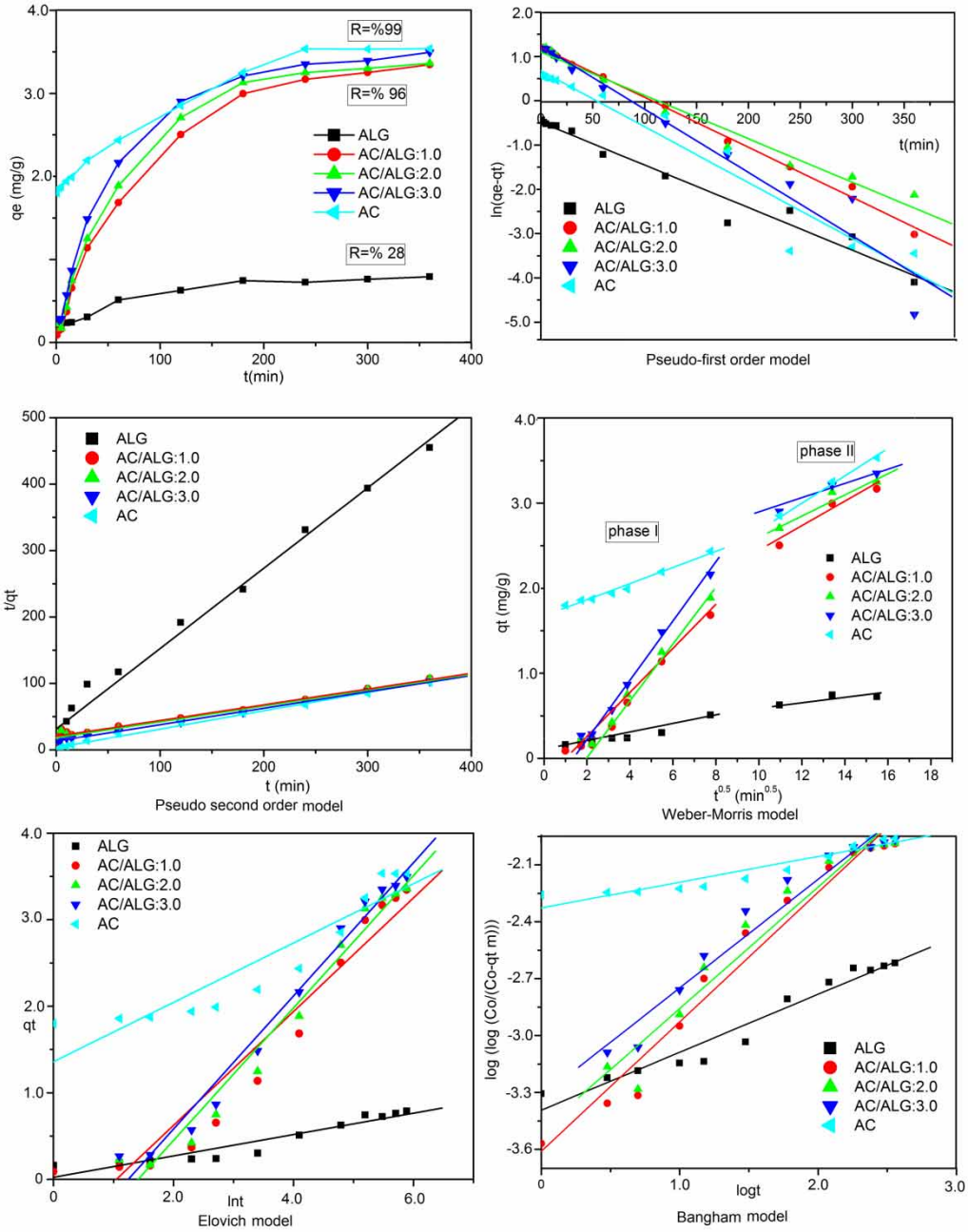

Figure 4 | Adsorption kinetic models of naproxen onto AC, ALG, and AC/ALG beads.

model is used for chemisorption in heterogeneous surfaces, and the Bangham model assumes pore diffusion controls in adsorption (Largitte & Pasquier 2016). The model equations for naproxen adsorption onto the beads are represented in Table 2.

The $q_{e,experimental}$ values were measured as 3.56, 1.02, 3.39, 3.48, and 3.50 mgg^{-1} for raw AC, raw ALG, and AC/ALG:(1.0–3.0), respectively. The $q_{e,model}$ values of the pseudo-first-order kinetic model were calculated as 4.76 mgg^{-1} for raw AC, 0.32 mgg^{-1} for raw ALG, and 16.0, 12.6, and 17.4 mgg^{-1} for AC/ALG:(1.0–3.0), respectively; R^2 values were determined to be between 0.94 and 0.99 (Table 2). The $q_{e,model}$ values were different from the $q_{e,experimental}$ values, so this model was not suitable for the kinetic approach of naproxen adsorption.

For the pseudo-second-order kinetic model, the difference between the values was acceptable when q_e values

Table 2 | Adsorption kinetic model parameters of naproxen onto AC, ALG, and AC/ALG beads

	AC	ALG	AC/ALG:1.0	AC/ALG:2.0	AC/ALG:3.0
$q_{e\text{-experimental}}$ (mgg^{-1})	3.56	1.02	3.39	3.48	3.50
Pseudo-first-order kinetic model	$\log(q_e - q_t) = \log q_e - \frac{k_1}{2.303}t$				
$q_{e,model}$ (mgg^{-1})	4.76	0.32	16.0	12.6	17.4
k_1 (min^{-1})	0.03	0.02	0.02	0.02	0.03
R^2	0.94	0.96	0.99	0.97	0.95
Pseudo-second-order kinetic model	$\frac{t}{q_t} = \frac{1}{k_2 q_e^2} + \frac{1}{q_e}t$				
$q_{e,model}$ (mgg^{-1})	3.62	0.82	4.23	4.18	4.05
k_2 ($gmg^{-1}\,min^{-1}$)	0.02	4E-08	0.0027	0.0032	0.0046
h ($mgg^{-1}\,min^{-1}$)	0.28	3E-08	0.05	0.06	0.08
R^2	0.99	0.98	0.98	0.98	0.99
Weber–Morris intraparticle diffusion model	$q_t = k_{id}t^{0.5} + C$				
k_{id1} ($mgg^{-1}\,min^{-0.5}$)	0.09	0.04	0.25	0.29	0.33
R^2	0.98	0.90	0.97	0.98	0.99
k_{id2} ($mgg^{-1}\,min^{-0.5}$)	0.08	0.018	0.10	0.07	0.07
R^2	0.82	0.80	0.89	0.85	0.92
Elovich kinetic model	$q_t = \frac{1}{\beta}\ln(\alpha\beta) + \frac{1}{\beta}\ln t$				
β (gmg^{-1})	2.91	8.10	1.52	1.30	1.29
α ($mgg^{-1}\,min^{-1}$)	18.05	0.15	0.23	1.19	0.22
R^2	0.87	0.90	0.92	0.96	0.97
Bangham kinetic model	$\log\left[\log\left(\frac{C_o}{C_o - q_t m}\right)\right] = \log\left(\frac{k_o m}{2.303V}\right) + \alpha\log t$				
k_0 (Lg^{-1})	8E-04	7E-05	4E-05	5E-05	8E-05
α	0.13	0.30	0.68	0.64	0.57
R^2	0.90	0.95	0.97	0.95	0.955

obtained from the model and experiments were compared (for raw AC $q_{e,experimental} = 3.56\ mgg^{-1}$ and $q_{e,model} = 3.62\ mgg^{-1}$; for raw ALG $q_{e,experimental} = 1.02\ mgg^{-1}$ and $q_{e,model} = 0.82\ mgg^{-1}$; for AC/ALG:3.0 $q_{e,experimental} = 3.50\ mgg^{-1}$ and $q_{e,model} = 4.05\ mgg^{-1}$). Furthermore, adsorption rate constants were found to be 0.28, 3×10^{-8}, 0.05, 0.06, and $0.08\ mgg^{-1}\,min^{-1}$ for raw AC, raw ALG, and AC/ALG:(1.0–3.0), respectively. The R^2 values were between 0.98 and 0.99 for all adsorbents. These results implied that the naproxen adsorption kinetic profile was represented better by the pseudo-second-order model than the others.

From Figure 4, two separate multilinear regions were obtained for raw AC, raw ALG, and AC/ALG:(1.0–3.0) beads, expressing different mass transfer mechanisms that occurred between the beads and naproxen molecules according to the accepted approach of the model. The first phase (first one hour) represented the boundary layer diffusion effect and mass transfer through the external surface of raw AC, raw ALG, and all beads. The second phase (after one hour) exhibited intraparticle diffusion and gradual mass transfer. According to Table 2, k_{id1} and k_{id2} for raw AC, raw ALG, and the beads showed that intraparticle diffusion rates were lower than the boundary layer mass transfer rate during naproxen adsorption. The k_{id1} and k_{id2} constants for raw AC, AC/ALG:2.0, and AC/ALG:3.0 were determined as $k_{id1} = 0.09\ mgg^{-1}\,min^{-0.5}$ and $k_{id2} = 0.08\ mgg^{-1}\,min^{-0.5}$; $k_{id1} = 0.297\ mgg^{-1}\,min^{-0.5}$ and $k_{id2} = 0.077\ mgg^{-1}\,min^{-0.5}$; and $k_{id1} = 0.33\ mgg^{-1}\,min^{-0.5}$ and $k_{id2} = 0.07\ mgg^{-1}\,min^{-0.5}$, respectively. These results demonstrated that the boundary layer mass transfer rate was higher 1.1-fold, 3.9-fold, and 4.7-fold than the interior mass transfer for AC/ALG:(1.0–3.0) beads, respectively.

The correlation coefficients (R^2) for the Elovich model were calculated to be between 0.87 and 0.97 and the initial adsorption rates of raw AC, raw ALG, and the beads increased sharply with embedding AC into raw ALG ($\alpha_{ALG} = 0.15\ mgg^{-1}\,min^{-1}$ and $\alpha_{AC/CS\text{-}PVA:3.0} = 0.221\ mgg^{-1}\,min^{-1}$). Therefore, the Elovich model was a good fit for naproxen adsorption.

For the Bangham model, the correlation coefficients R^2 were calculated to be in the range of 0.90–0.97, and pore diffusion played a significant role during naproxen adsorption.

Adsorption thermodynamic

Thermodynamic studies of naproxen adsorption onto AC/ALG beads were carried out at three different temperatures to provide information on adsorption-related internal energy changes (Ogata *et al.* 2017). The temperature effect of naproxen adsorption onto AC/ALG beads is shown in Figure 5(a). Naproxen adsorption onto raw AC and AC/ALG:(1.0–3.0) beads was spontaneous with negative values of Gibbs free energy (ΔG^o); in contrast, the ΔG^o value was positive for only raw ALG, and the adsorption process onto raw ALG was non-spontaneous, and this situation is generally unexpected. ΔH^o values of naproxen adsorption onto raw AC, raw ALG, and AC/ALG:(1.0–3.0) were calculated as 2,770, 5,770, 1,090, 1,690, and 3,260 $Jmol^{-1}$, respectively, indicating the naproxen adsorption onto all adsorbents was endothermic in nature. According to Table 3, positive ΔH^o values showed an endothermic reaction, so an increase in temperature supported the adsorption. The endothermic behaviour of adsorption was confirmed by positive values of enthalpy, and positive/negative enthalpy values represented the classified chemical ($\Delta H^o > 35{,}000\ Jmol^{-1}$) or physical ($\Delta H^o < 35{,}000\ Jmol^{-1}$) adsorption. Therefore, naproxen adsorption using AC/ALG beads was a physical adsorption process. ΔS^o values were determined as 70.7, 13.9, 28.1, 35.9, and 43.5 $Jmol^{-1}\ K^{-1}$ for raw AC, raw ALG, and AC/ALG:(1.0–3.0), respectively, and positive values demonstrated the disorderliness, irregularity, and conformational entropies of the beads and that the naproxen interface increased during the adsorption process.

Desorption, reusability, and adsorption mechanism

The loaded naproxen was desorbed from the surface of the AC/ALG:3.0 beads by distilled water, ethanol, and

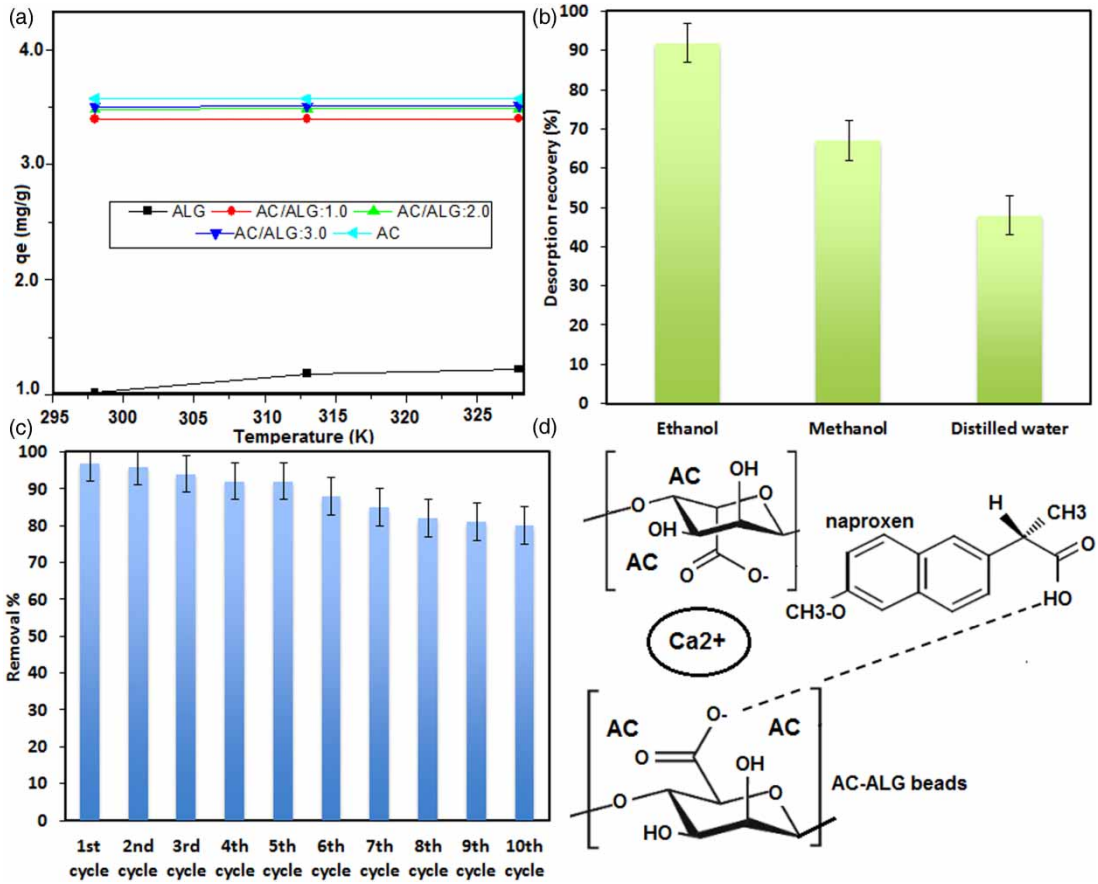

Figure 5 | Desorption, reusability, and adsorption mechanism of naproxen.

Table 3 | Thermodynamical parameters of naproxen adsorption onto AC, ALG, and AC/ALG beads

Adsorbent	ΔG^0(Jmol^{-1}) 298 K	313 K	328 K	ΔH^0(Jmol^{-1})	ΔS^0(Jmol^{-1} K^{-1})
AC	−17,830	−19,370	−20,430	2,770	70.7
ALG	1,610	1,400	1,190	5,770	13.9
AC/ALG:1.0	−7,300	−7,730	−8,140	1,090	28.1
AC/ALG:2.0	−9,030	−9,590	−10,100	1,690	35.9
AC/ALG:3.0	−9,720	−10,360	−20,420	3,260	43.5

methanol over five hours to ensure that equilibrium was obtained. This investigation showed (Figure 5(b)) that ethanol was able to desorb naproxen from the AC/ALG:3.0 beads with the highest efficiency in comparison with the other eluting solvents. This was related to the high solubility of naproxen in ethanol. Thus, ethanol was utilized as a desorption solvent in the subsequent experiments.

AC/ALG:3.0 beads were examined for reusability for ten consecutive cycles. Almost 94% desorption efficiency was achieved using ethanol in the third cycle. The beads in the seven consecutive cycles showed a high performance and the beads adsorbed nearly 85% of the naproxen even in the seventh cycle (Figure 5(c)). Naproxen removal % values remained nearly constant for seven cycles and high capacities for the beads during the adsorption–desorption processes were obtained. It can be safely stated that no significant differences occurred in the adsorption capacity of the beads after the seventh cycle.

Considering all preliminary adsorption experiments, the plausible adsorption mechanism between naproxen and AC/ALG beads can be explained with characteristics of carbonaceous adsorbents (Simsek *et al.* 2017). The most important factor that affected naproxen adsorption was the hydrogen-bond interaction between AC/ALG beads and naproxen molecules (Figure 5(d)). The hydrogen bonding between the O-H group in naproxen and the C-O-O$^-$ groups of the AC/ALG beads could be involved in the adsorption.

CONCLUSION

Among various adsorbents used to adsorb pharmaceuticals in wastewater, AC is one of the most-used adsorbents due to its high surface area, pore size distribution and adsorption capacity. Therefore, the highly porous structure and large specific surface area of AC and the tunable surface properties and adsorption performance of ALG can be combined to prepare an efficient adsorbent for the adsorption of pharmaceuticals from wastewater.

In the current study, AC/ALG beads were fabricated and applied for adsorption of the nonsteroidal anti-inflammatory drug naproxen from wastewater. The introducing of AC into the alginate's molecular structure significantly enhanced the surface area and pore size of the polymer and improved the adsorption capacity; therefore, AC/ALG beads effectively eliminated 98.0% of the naproxen. The investigation results were best described by the Freundlich, Temkin, and D-R models, the pseudo-second-order model appeared to be more suitable to describe the adsorption, and the adsorption executed a spontaneous and endothermic process. Regeneration studies indicated that AC/ALG beads could successfully retain naproxen after seven cycles.

FUNDING

The financial support provided by Yalova University Scientific Research Projects Coordination Department (Project no: 2017/DR/002) is gratefully acknowledged.

REFERENCES

Ahmed, M. J. & Hameed, B. H. 2018 Removal of emerging pharmaceutical contaminants by adsorption in a fixed-bed column: a review. *Ecotoxicology and Environmental Safety* **149**, 257–266.

Dada, A. O., Olalekan, A. P., Olatunya, A. M. & Dada, O. 2012 Langmuir, Freundlich, Temkin and Dubinin–Radushkevich isotherms studies of equilibrium sorption of Zn^{2+} onto phosphoric acid modified rice husk. *IOSR Journal of Applied Chemistry* **3** (1), 38–45.

Hu, Z. H., Omer, A. M., Ouyang, X. K. & Yu, D. 2018 Fabrication of carboxylated cellulose nanocrystal/sodium alginate hydrogel beads for adsorption of Pb(II) from aqueous solution. *International Journal of Biological Macromolecules* **108**, 149–157.

İlbay, Z., Şahin, S., Kerkez, Ö. & Bayazit, Ş. S. 2015 Isolation of naproxen from wastewater using carbon-based magnetic adsorbents. *International Journal of Environmental Science and Technology* **12**, 3541–3550.

Inyinbor, A. A., Adekola, F. A. & Olatunji, G. A. 2016 Kinetics, isotherms and thermodynamic modeling of liquid phase adsorption of Rhodamine B dye onto *Raphia hookerie* fruit epicarp. *Water Resources and Industry* **15**, 14–27.

Khazri, H., Ghorbel-Abid, I., Kalfat, R. & Trabelsi-Ayadi, M. 2017 Removal of ibuprofen, naproxen and carbamazepine in aqueous solution onto natural clay: equilibrium, kinetics, and thermodynamic study. *Applied Water Science* **7**, 3031–3040.

Kooijman, G., de Kreuk, M. K., Houtman, C. & van Lier, J. B. 2020 Perspectives of coagulation/flocculation for the removal of pharmaceuticals from domestic wastewater: a critical view at experimental procedures. *Journal of Water Process Engineering* **34**, 101161.

Largitte, L. & Pasquier, R. 2016 A review of the kinetics adsorption models and their application to the adsorption of lead by an activated carbon. *Chemical Engineering Research and Design* **109**, 495–504.

Larosa, C., Salerno, M., de Lima, J. S., Merijs Meri, R., da Silva, M. F., de Carvalho, L. B. & Converti, A. 2018 Characterization of bare and tannase-loaded calcium alginate beads by microscopic, thermogravimetric, FTIR and XRD analyses. *International Journal of Biological Macromolecules* **115**, 900–906.

Larous, S. & Meniai, A. H. 2016 Adsorption of Diclofenac from aqueous solution using activated carbon prepared from olive stones. *International Journal of Hydrogen Energy* **41** (24), 10380–10390.

Li, C., Lu, J., Li, S., Tong, Y. & Ye, B. 2017 Synthesis of magnetic microspheres with sodium alginate and activated carbon for removal of methylene blue. *Materials* **10**, 84.

Ogata, F., Ueta, E., Toda, M., Otani, M. & Kawasaki, N. 2017 Adsorption of phosphate ions from an aqueous solution by calcined nickel–cobalt binary hydroxide. *Water Science & Technology* **75** (1), 94–105.

Önal, Y., Akmil-Başar, C. & Sarıcı-Özdemir, Ç. 2007 Elucidation of the naproxen sodium adsorption onto activated carbon prepared from waste apricot: kinetic, equilibrium and thermodynamic characterization. *Journal of Hazardous Materials* **148** (3), 727–734.

Reynel-Avila, H. E., Mendoza-Castillo, D. I., Bonilla-Petriciolet, A. & Silvestre-Albero, J. 2015 Assessment of naproxen adsorption on bone char in aqueous solutions using batch and fixed-bed processes. *Journal of Molecular Liquids* **209**, 187–195.

Saloglu, D. & Ozcan, N. 2018 Activated carbon embedded chitosan/polyvinyl alcohol biocomposites for adsorption of nonsteroidal anti-inflammatory drug-naproxen from wastewater. *Desalination and Water Treatment* **107**, 72–84.

Seo, P. W., Bhadra, B. N., Ahmed, I., Khan, N. A. & Jhung, S. H. 2016 Adsorptive removal of pharmaceuticals and personal care products from water with functionalized metal–organic frameworks: remarkable adsorbents with hydrogen-bonding abilities. *Scientific Reports* **6**, 34462.

Simsek, E. B., Saloglu, D., Ozcan, N., Novak, I. & Berek, D. 2017 Carbon fiber embedded chitosan/PVA composites for decontamination of endocrine disruptor bisphenol-A from water. *Journal of Taiwan Institute of Chemical Engineers* **70**, 291–301.

Yu, Z., Peldszus, S. & Huck, P. M. 2008 Adsorption characteristics of selected pharmaceuticals and an endocrine disrupting compound – Naproxen, carbamazepine and nonylphenol – on activated carbon. *Water Research* **42**, 2873–2882.

Zhou, X. & Zhou, X. 2014 The unit problem in the thermodynamic calculation of adsorption using the Langmuir equation. *Chemical Engineering Communications* **201**, 1459–1467.

First received 9 December 2019; accepted in revised form 10 April 2020. Available online 24 April 2020